International Journal of GEOMATE, June 2023, Vol. 24, Issue 106, pp.111-119
ISSN: 2186-2982 (P), 2186-2990 (O), Japan, DOI: https://doi.org/10.21660/2023.106.3281
Geotechnique, Construction Materials and Environment

SEISMIC RESPONSE ANALYSIS OF A LAYERED SOIL COLUMN UNDER DIFFERENT WATER CONDITIONS

Laura Ibagon[1,2], Bernardo Caicedo[1], Diego Camacho[2], *Juan P. Villacreses[1,2], Fabricio Yépez[2].

[1]Universidad de los Andes, Colombia; [2]Colegio de Ciencias e Ingenierías, Universidad San Francisco de Quito, Ecuador.

*Corresponding Author, Received: 01 Feb. 2022, Revised: 01 Jan. 2023, Accepted: 24 March 2023

ABSTRACT: The seismic site effect is influenced by the soil's dynamic properties. These properties are affected by the soil´s water content, which varies according to climatic conditions. This work aims to analyze the seismic site effect of a thirty-meter soil column which has different water table levels. An evaporation simulation is conducted on these columns. The mechanical properties under different suction pressures were obtained from previous research. Then, a finite-difference model was used to simulate the soil-environment interaction and the results were applied to build the water profiles of the column. Finally, a finite element model was used to simulate the seismic response at the top of the deposit. The results showed a remarkable difference in soil response according to the degree of saturation of the column. The change in saturation due to climate conditions does not have a significant effect. On the other hand, the results showed that the water table level affects the response of the deposit. The deposit with dryer conditions had a greater response acceleration in the surface than the deposit in a wetter state. This work opens many research possibilities, where the influence of water content and climate conditions in soil's mechanical and dynamical properties can be studied. These investigations would help achieve a better understanding of soil behavior and its interaction with the environment.

Keywords: Seismic site effect, Shear modulus, Partial saturation, Water table level, Evaporation.

1. INTRODUCTION

The seismic site response of a site is strongly affected by the geological conditions of the location. Concerns about seismic wave amplification have increased because of many natural disasters over the last decades. The 1985 Mexico City earthquake is a perfect example of site amplification, producing thousands of casualties and great structural damage because of seismic amplification. After this event, earthquake engineers recognized the importance of understanding local amplification to prevent human and material damage [1].

Modeling and understanding the seismic site effect has had significant development in the past decades. Research has focused on modeling soil properties and more realistic configurations. These analyses commonly use damping, soil density, and dynamic properties (i.e., shear modulus) as their main inputs to compute the seismic site response. Nevertheless, soil properties are not uniform, and studies suggest that changing water content has a significant effect on soil dynamic resistance. To support this idea, Villacreses et al. [2] and [3] state that the structural stiffness of a soil structure changes due to the water pressure inside de soil skeleton [2]. Furthermore, climatic conditions can alter water content in the soil structures. To the best of the author's knowledge, there is little research that considers different water contents and changing properties due to climate conditions in seismic site effect. Therefore, this investigation explores this area for a better understanding of the influence of water content in seismic response analysis.

In this investigation, the seismic response analysis of a layered soil column will be assessed. Two factors will be analyzed as parameters that affect seismic response analysis: water table level and changing climate conditions expressed in terms of evaporation. To achieve this objective, the material properties of the soil at different suction pressure values were obtained from the literature [2] and [3]. A finite-difference model was used to simulate an evaporation process of the soil deposit [2]. Finally, a finite-element model was used to assess the seismic wave propagation along a one-dimensional soil column [4].

2. RESEARCH SIGNIFICANCE

This investigation explores the effect of partial saturation in seismic wave propagation in a soil deposit. Two mechanisms to change the pore water pressure are explored. The first mechanism is water table level, and the second is evaporation due to climate variables. This research aims to contribute to the understanding of the effect of partial saturation in unsaturated conditions. Three seismic signals were selected to evaluate the influence of the frequency content of the input motion.

3. MATERIALS

3.1 Material Properties

This investigation evaluates a soil deposit of fine-grained soil. The properties are shown in Table 1 and they were determined in [3] and [2]. The soil was classified using the Unified Soil Classification System (USCS) as a high plasticity clay (CH). The Soil Atterberg Limits are a liquid limit of 87% and a plastic limit of 37%. Fig. 1 shows the grain size distribution of the studied material, The percentile values D_{30}, $D_{50,}$ and D_{90} are $1.5\mu m$, $2.5\mu m$ and $9\mu m$. Additionally, the dry density of the material is 1.35 g/cm3. The properties are summarized in Table 1.

Table 1 Soil Properties

Plastic Limit (%)	37
Liquid Limit (%)	87
Water Content (%)	31.3
Dry Density (g/cm^3)	1.35
D30 (μm)	1.5
D50 (μm)	2.5
D90 (μm)	9

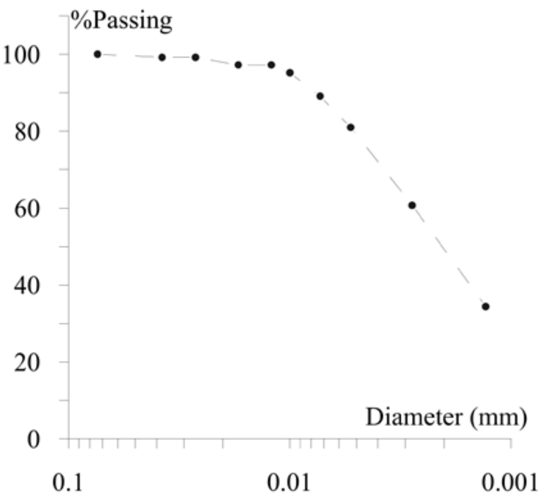

Fig.1 Particle size distribution of soil

3.2 Water Retention Curve (WRC)

The soil's mechanical properties vary according to the degree of saturation. For this reason, it is pertinent to study the relationship between the water retention curve and the mechanical properties. The methodology to measure the WRC is described meticulously in [3], and the results are presented in Fig. 2. The WRC was measured in the drying path. Samples were conditioned in a relative humidity environment of 52.4%. These samples were left for varied periods ranging from a few minutes up to two days. The residual water content of 3% was achieved at the end of the conditioning process. A chilled mirror hygrometer was used to measure the suction pressure (ψ). The degree of saturation (Sr) was computed using the specific gravity of the soil and the volumetric information of the samples throughout the conditioning process [5]. Fig. 2. shows the water retention curve of the soil material [3]. The soil´s suction increases from 10^3 kPa to 10^4 kPa when the degree of saturation decreases from 70% to 20%. This change of matric suction increases the effective stress in the sample, which modifies the mechanical response of the soil.

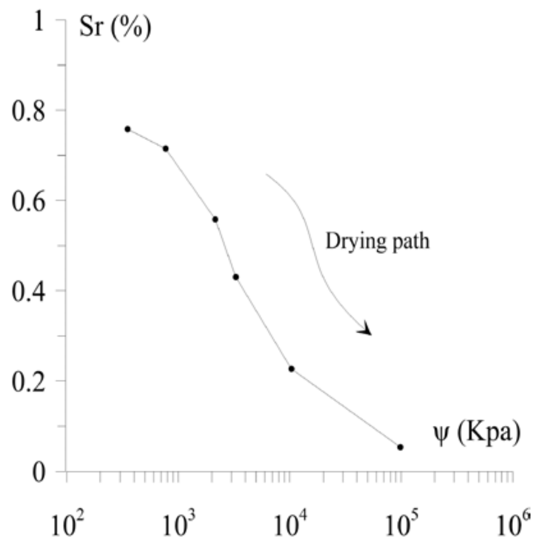

Fig. 2 (WRC) Water retention curve [3].

4. METHODS

The following section provides the methodology used in this investigation. The gathered information and data collection from [3], [2], and [6] are presented. Also, the section shows the procedure used to simulate water evaporation and the finite element model used for site response analysis of soil deposits.

4.1 Rheometer

The mechanical properties of the soil under different degrees of saturation were used in a numerical simulation. The simulation seeks to evaluate the performance of a soil deposit under changing weather conditions. Villacreses et al. [2] presented an experimental procedure to determine dynamic shear modulus and damping coefficients using a Torsional Dynamic Shear Rheometer. The procedure uses cylindrical 1.3cm diameter soil specimens, with a 4.0cm height. The samples are conditioned in a controlled relative humidity using the air-drying technique. Finally, the sample´s base is fixed, and the top is subjected to a sinusoidal torsional loading scheme. Suction is measured after every torsional test, applying the hygrometer method described in [3] and [5].

4.2 Climate Chamber

Soil´s water content and its mechanical properties are directly influenced by changing weather conditions. To study these climate effects on soil´s water content, Lozada et al. [7] designed a climatic chamber. This instrument is capable of simulating variables such as wind velocity, solar irradiance, atmospheric pressure, and relative humidity. In this investigation, soil samples were subjected to a temperature of 40°C and a wind velocity of 1.2 m/s. A digital scale incorporated in the device allowed to measure evaporation. These evaporation rates were used to estimate the soil´s water content evolution during a drying process. The results can be found in [2].

4.3 Finite Difference Model

Using the results of the rheometer test and the water flux measured in the climatic chamber, a numerical simulation was conducted. A finite-difference simulation is used to compute the water profile during drying and wetting scenarios [2]. The model considered two assumptions: porosity is constant over time and flow in the vapor phase is neglected. The finite-difference model used the continuity equation of water flow in unsaturated soils, given in Eq. (1)

$$n\frac{\partial S_r}{\partial t}+\nabla\cdot(-k_w(S_r)\,\nabla\psi)=0 \qquad (1)$$

Where (Sr) represents de degree of saturation, (t) time, (n) soil´s porosity, (ψ) total potential and (k_w) water conductivity of the liquid phase. Then, a forward difference time operator and the central difference two-dimensional space operator in Eq. (1) permitted a time and space domain discretization. Thus, discretized continuity equation allowed the construction of Eq. (2) which describes the evolution of soil´s total potential in time. The time variation of saturation (Sr) has a relationship with time suction variation (s). Thus the position of the spatial discretization is constant over time, and the total potential (ψ) is the suction. [2]. The water-specific water capacity of the soil C_θ was obtained from [2].

$$n\frac{\partial S_r}{\partial t}=C_\theta\frac{\partial s}{\partial t}=C_\theta\frac{\psi_{i,j}^{t+\Delta t}-\psi_{i,j}^{t}}{\Delta t} \qquad (2)$$

4.4 Finite Element Model for Site Response Analysis of Soil Deposit

4.4.1 Model Description

A finite element simulation is used to analyze the seismic response of a soil deposit. The model used in this research was obtained from an investigation conducted by McGann & Arduino [4]. This model computes the reaction of a one-dimensional soil column which is divided into layers. The finite element model uses a Pressure Independent Multi-yield material to simulate the behavior of undrained clays. The column is subjected to an earthquake ground motion to compute the surface response.

The simulation computes the seismic response for a 30 meters depth soil deposit. This depth was selected because the local regulations establish geotechnical exploration to this depth for seismic analysis [8]. The soil deposit profile is divided into thirty layers of one meter each. This deposit overlies a bedrock that has a shear wave velocity of 1524 m/s. The model implements Lysmer-Kuhlemeyer's dashpot at the base of the soil profile, deeply explained in [4] and [6]. Fig. 3 shows the mesh and nodes used for the model. Fig. 3 shows that for n elements, there are $2n+1$ nodes. These nodes are numbered by a left-to-right, top-to-bottom system. Nodes 1 and 2 nodes are fixed against y-direction displacements. Nodes from node 3 to node 2n+2 are tied together using an equal degree of freedom command. Extended information about the model description can be found in [4].

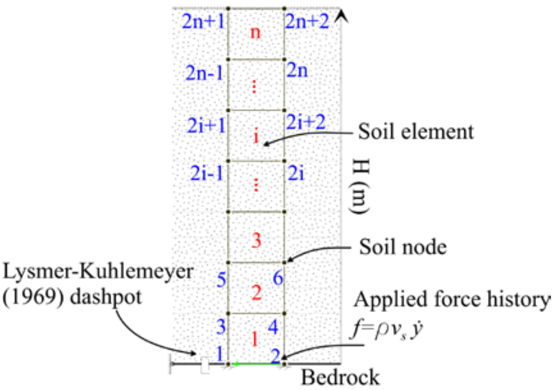

Fig. 3 Visual representation of finite element site response model. [4]

4.4.2 Soil Material Properties

The mechanical behavior of the soil computed in the finite element model required shear wave velocity, Poisson ratio, and effective stress. The following sub-section shows several inputs needed for the model and how these were obtained.

4.4.2.1 Poisson Ratio

Poisson's ratio (ν) allows the calculation of some elastic and mechanical parameters of the soil. Commonly, it is taken as constant for both unsaturated and saturated soils. Nevertheless, water content has a significant effect on this parameter in fine-grained soils. This means that Poisson´s ratio has a relationship with the degree of saturation. Oh et al. [9] propose an experimental relationship between Poisson's ratio (ν) and the degree of saturation (Sr) for fine-grained soils. For the numerical model, Poisson's ratio was obtained for each layer using Oh´s relationship.

4.4.2.2 Soil Shear Wave Velocity

Soil´s shear wave velocity was computed using Eq (3), where (G) is the soil´s shear modulus and (ρ) is the soil´s density. Both properties were obtained using the rheometer and climate chamber tests performed in [2] and [7]. The results were then interpolated for each suction value.

$$V_s = \sqrt{\frac{G}{\rho}} \tag{3}$$

From these values, Young (E) and bulk modulus (B) were obtained using Eq (4) and Eq (5) respectively.

$$E = 2G(1+\nu) \tag{4}$$

$$B = \frac{E}{3(1-2\nu)} \tag{5}$$

4.4.2.3 Effective Stress

Effective stress is important when computing the dynamic response of a soil deposit subjected to combined effects of confinement stress and suction pressure. Equation (6) shows Bishop´s approach to determining effective stress. This expression is explained in [10] and was used for this investigation.

$$\sigma' = (\sigma - u_a) + \chi(u_a - u_w) \tag{6}$$

Where σ' is the effective stress, $(\sigma - u_a)$ is the net stress, $(u_a - u_w)$ is the matric suction and χ is the effective stress parameter. For this investigation, the matric suction is assumed to be the same as the suction pressure. The effective stress parameter (χ) is a value related to the soil structure and it is used to describe the change in effective stress. Multiple attempts have tried to quantify χ theoretically and experimentally. One of these approaches, shown in Eq (7), presents the best fit for an experimental relationship between χ and suction, as proposed in [11].

$$\chi = \left[\frac{(u_a - u_w)}{(u_a - u_w)_b}\right]^{-0.55} \tag{7}$$

In this equation, $(u_a - u_w)_b$ is the suction for the air entry value, and this investigation adopts a value of 0.42 MPa for this parameter [3]. The equation shows that χ acquires a value of *0* for dry soils and *1* for saturated soils. This effective stress approach allowed the finite element model to determine the effective stress values for different depths, saturation, and suction values in the soil deposit.

4.4.3 Seismic Motion

The model applied earthquake ground motions at the base of the soil column to analyze seismic wave propagation [12, 13, 14]. In this investigation, three seismic acceleration records from PEER NGA database were used. Signals were selected due to the rock conditions of the sites and the different predominant frequencies. Fig. 4 shows the accelerograms and the Fourier Spectra of the 3 records (Loma Prieta 1989 earthquake Gilroy N°1 E-W station, Kobe 1995 Kobe University station, and Loma Prieta 1989 Piedmont Jr High School station). The last record was amplified 5.8 times the original signal [15].

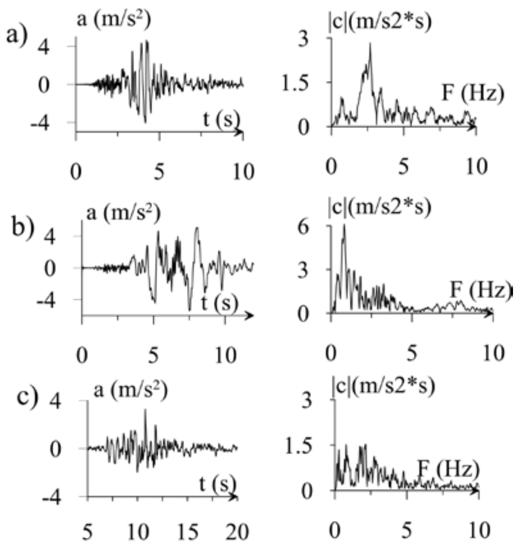

Fig. 4 Ground motion acceleration and FFT a) 1989 Loma Prieta earthquake Gilroy N°1 E-W b) amplified 1995 Kobe earthquake and c) amplified 1989 Loma Prieta earthquake Piedmont Jr station.

5. RESULTS AND DISCUSSION.

In the next section, the results are discussed in the following order: first, results obtained in [3] and [2] were analyzed to construct new relationships. Second, the results from the finite difference simulations were used to calculate the different water contents depending on the soil deposit depth. Finally, the seismic response was assessed through the finite element model using the three described ground motions. These results aim to understand de seismic response of a soil column under different water contents.

5.1 Material Properties (Climate Chamber, Rheometer).

Fig. 2 shows the relationship obtained between suction pressure (ψ) and the degree of saturation (Sr), known as the soil-water characteristic curve. In this Fig. 2, suction pressure increases as the water content within the soil reduce [16].

Fig. 5 illustrates the relationship between the degree of saturation (Sr) and soil´s bulk density (γ_b). The information to construct the graph was obtained from the investigation of [2]. Fig. 5 shows that bulk density increases as water content does. For instance, Fig. 5 shows that bulk density increases from 14.5 kN/m^3 to 17 kN/m^3 as the degree of saturation increases from 0.22 to 0.75. The bulk density measure the amount of water inside the soil skeleton. For later computations, this weight is going to be assigned to specific parts of the soil deposit. It is important to mention that the material model uses as input parameters the shear modulus and density of the material.

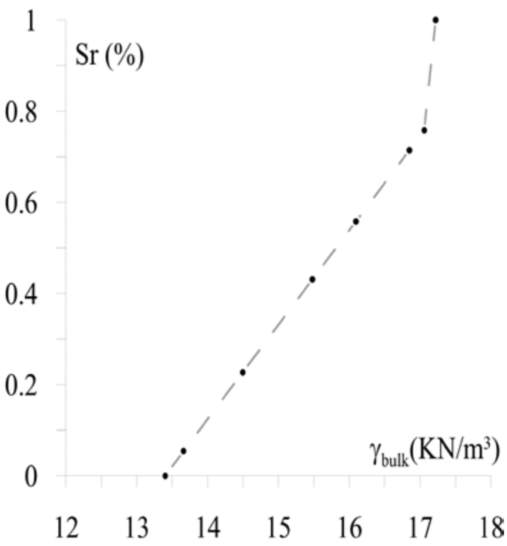

Fig. 5 Degree of saturation as a function of bulk density.

The maximum shear modulus is proportional to effective stress. These values were measured in [2] and used in this research. Suctions in these samples were transformed into effective stress. In [2] the suction pressure was transformed to effective stress using Eq.6 and Eq.7. Fig. 6 illustrates the relationship between the maximum shear modulus (G) and the effective stress (σ'). Fig. 6 shows that shear modulus increases as effective stress does. However, Fig. 6 shows that for effective stress values below 550 KPa, there is no remarkable change in the maximum shear modulus.

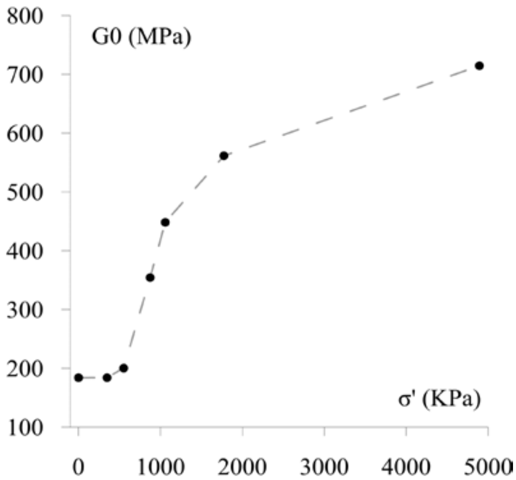

Fig. 6 Relationship between the shear modulus (G) and the effective stress (σ´).

The finite element model used in this investigation defines yield surfaces based on shear modulus reduction curves. The shear modulus reduction curves were measured in [2] for different water contents. Fig. 7 illustrates the soil´s modulus reduction curves (G/G_{max}) vs shear strain (ε) for multiple suction pressure values. Fig. 6 shows that at suction pressure above 10 MPa, the degradation of the shear modulus degradation curve changes radically. Fig. 7 shows that the shear modulus reduces as shear strain increases. For example, when the shear strain increases from 0.0001 to 0.001, most of the curves show degradation of almost 50% of the maximum shear modulus. The finite element model used these modulus reduction curves to compute the surface motion. Intermediate values were linearly interpolated for different suction pressure values.

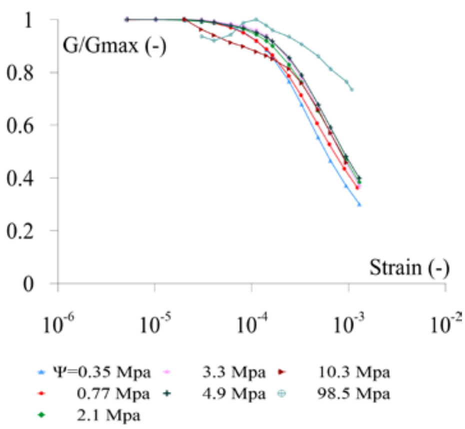

Fig. 7 Modulus reduction curves for multiple suction pressures.

5.2 Finite-Difference Simulation (Water Table Level and Evaporation)

Finite-difference simulations were carried out in thirty meters soil columns, using different water table levels (i.e., 5, 15, and 25m). The simulation provides the relationship between the saturation degree (*Sr*), water pressure (*Uw*), and depth of soil deposit (*H*). Later, the numerical and experimental results were used to compute the bulk density (γ_b) for different depths along the soil strata [3], [2]. For this investigation, the numerical results of the evaporation for simulation's times of 0, 600, and 87600 hours were used. These profiles were selected because they show a noteworthy difference in effective stress distribution. Fig. 8 shows the relationships obtained from the simulations, showing the variations in (*Sr*) and (*Uw*) along with the soil depth. These results consider the different water table levels and constant climatic conditions. The results show that bulk density rapidly changes as depth reaches water table level. Indeed, bulk density increases from 13.65 kN/m^3 to 17.22 kN/m^3 as the soil becomes saturated. Bulk density behaves like a straight line after the first 5 meters. On the other hand, the Fig. illustrates that the degree of saturation slowly increases with depth until it reaches total saturation at the water table level. Also, the Fig. shows the difference in water pressure values depending on the water table level. For example, water pressure at the beginning is 43.61 MPa when the water table level is 5m depth and 239.61 MPa when the water table level is at a 25m depth. These results show that water pressure is greater when the water table level is deeper. Furthermore, 87600 hours of evaporation have a significant effect on water pressure values on the first meters of soil deposit.

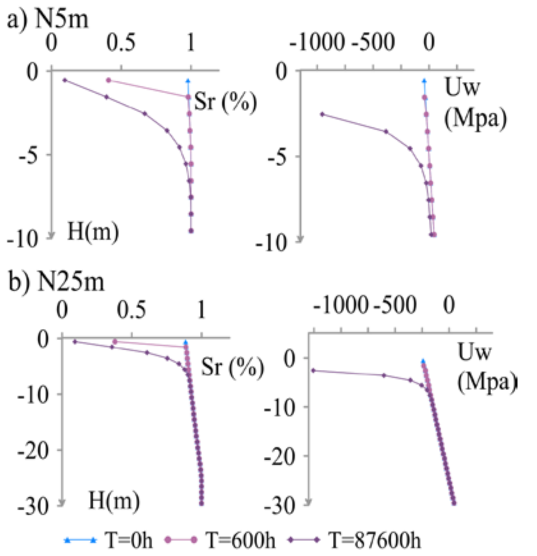

Fig. 8 relationship between the degree of saturation (*Sr*), water pressure (*Uw*), and depth of soil deposit (*H*) for 0, 600, and 87600 hours of the evaporation process and water table levels of a)5m and b)25m

For the seismic site effect, the most common mechanical properties are the shear modulus (G) and the shear wave velocity (V_s). Fig. 9 illustrates the relationship between soil´s mechanical properties and depth for different water table levels. Fig. 9a shows the results for a water table level of 5m, and Fig. 9b for 25m. These relationships are presented for 0, 600, and 87600 hours of the evaporation process. As presented in Fig. 9, both shear modulus and shear wave velocity do not have a remarkable change regarding water table level. The Fig. shows that the shear modulus remains virtually constant at a value of approximately 184.10 MPa after the first 5m. For instance, effective stress changes from 150 kPa to 350 kPa, which implies a variance in shear modulus of less than 0.11 MPa.

Fig. 9 evidence the change in the shear modulus for different piezometric levels. The shear modulus changes in the first meters of soil depth as a function of water evaporation. As an example, for a depth of 1.55 m, the shear modulus is almost 3 times bigger after an 87600-hour of evaporation than its original state. Fig. 9a and 9b show that shear wave velocity has almost the same values at the top of the deposit. Nevertheless, Fig. 9b shows that shear wave velocity does have a notable difference at the bottom of the deposit. As an example, the shear wave velocity is 323.82 m/s for a water table level of 5m and 20 depth. Whereas the shear wave velocity is 326.81 m/s for water table level 25m and the same depth. These results change for a depth of 29.5m achieved at the end of evaporation since shear wave velocity is 323.84 m/s for a water table level of 5m and 331.86 m/s for a water table level of 25m.

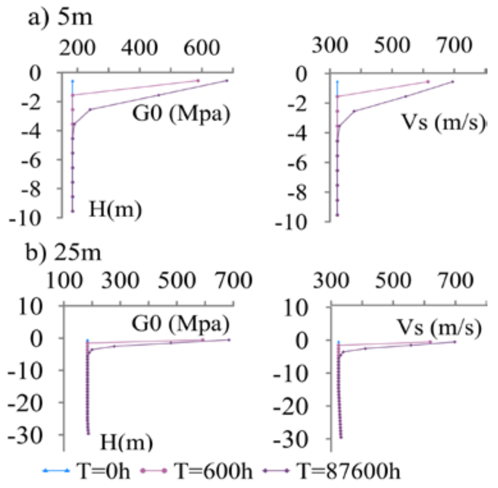

Fig. 9 relationship between a) shear modulus, shear wave velocity, and depth for a 5m water table level and b) shear modulus, shear wave velocity, and depth for a 25m water table level for different water table levels for 0, 600, and 87600 hours of the evaporation process

5.3 Seismic Response

The previous results showed the difference in the mechanical properties of soil according to the depth, water table levels, and evaporation conditions of the deposit. Once obtained these results, the finite element model was used along with 3 earthquake motions at the base of the deposit (Fig. 4). The unidimensional wave propagation allows the seismic response at the top of the soil deposit to be computed. The period of the soil deposit was estimated, and this value ranges between 0.35 and 0.37 seconds depending on the water table level and the climate condition imposed. Additionally, the surface response accelerograms were used to compute acceleration response spectrums for a simple oscillator with a variable natural period.

Fig. 10 illustrates the acceleration response spectrum at the top of the soil column obtained from introducing the 1995 Kobe earthquake signal. Also, Fig. 10 shows the different outcomes considering distinct water table levels (i.e., 5, 15, 25m), and 0 and 87600 hours of evaporation. The following analyses will focus on the effects of water table level and climate conditions on the seismic response. Starting with the effects of climate conditions, Fig. 10 shows that evaporation does not have a significant effect on the seismic response of the soil deposit. For example, the response spectrum of the 5m water table shows that the maximum acceleration for the 0 hours is 18.39 m/s^2 whereas for the 87600 hours is 18.31 m/s^2. Thus, a 10-year evaporation span produces a percentual difference of 0.4% in the maximum acceleration response. Analyzing the effects of the water table level, Fig. 10 shows that the water table modifies the response of the soil deposit. Notably, the results reveal that the acceleration increase as the depth of the water table level does. As an example, when the period of the oscillator is close to the period of the deposit, the bedrock acceleration is 11.45 m/s^2. This value is amplified to 17.98 m/s^2 when the water table level is at 5m and amplified to 18.66 m/s^2 when the water table level is at 25m. Therefore, the results show that the acceleration response has a percentual increase of 3.78%. This amplification can be explained by analyzing the Fourier Spectrum of the signal shown in Fig. 4b. The figure shows that the frequency content of the signal ranges from 0.2 Hz and 3.2 Hz. Thus, for values close to the natural frequency of the deposit, and due to the significant frequency content in the record, amplification can take place.

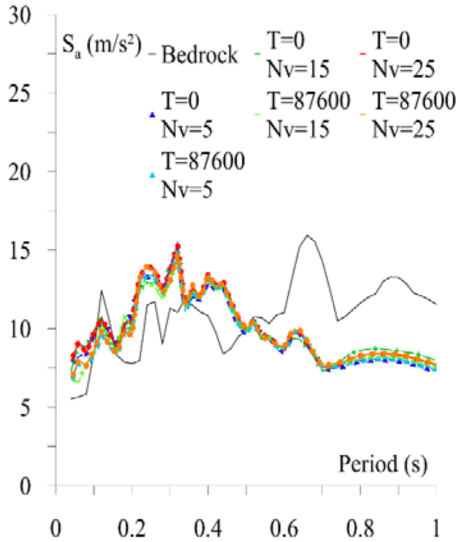

Fig. 10 1995 Kobe earthquake acceleration response spectrum at top of the deposit for different water table levels (i.e., 5, 15, 25m) and exposed to 0 and 87600 hours of evaporation.

Fig. 11 shows the response acceleration spectrum obtained from introducing the Loma Prieta - Piedmont station signal in the model. Fig. 11 shows similar results to those obtained previously with the Kobe signal. Starting with the effects of climate conditions, Fig. 11 shows that the evaporation process in this deposit does not have a remarkable difference in the acceleration response of the signal. For instance, using an oscillator period of 0.36 seconds and a water table level of 5 m, the acceleration response is 8.34 m/s^2 at the beginning and 8.57 m/s^2 after 87600 hours of evaporation. These results show that, for this period, the climate conditions had a percentual difference of 2.7% in the acceleration response. Analyzing the effects of the water table level, Fig. 11 shows that the water table modified the response of the soil deposit. Fig. 11 shows that, for a water table level of 5m, and a period of 0.34s, the acceleration response is 8.46 m/s^2 whereas for a water table level of 25m the acceleration response is 9.15 m/s^2. These results show that, for this period, the water table level produces a percentual difference of 8.15%. Additionally, Fig. 11 shows that when the oscillator and the deposits period are matched, the species' structural acceleration greater amplified. This amplification increases as the water table level became deeper. The Fourier spectrum of the signal in Fig. 4c shows that the frequency content of the motion is relatively uniform. The amplification of the signal takes place since there is significant frequency content for values close to the natural frequency of the deposit.

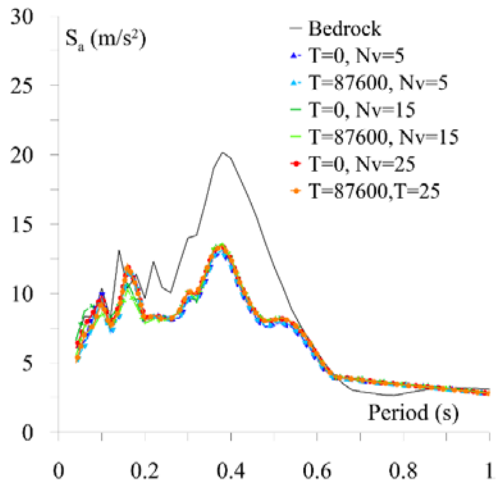

Fig. 11 1989 Loma Prieta (Piedmont station) acceleration response spectrum at top of the deposit for different water table levels (i.e., 5, 15, 25m) and exposed to 0 and 87600 hours of evaporation.

The acceleration response spectrum obtained from introducing the Loma Prieta Gilroy station signal is shown in Fig. 12. It is important to observe in the figure the remarkable difference in the response in comparison to the previous signals. This figure shows a strong reduction in the acceleration response at the top of the deposit. First, the effects of the evaporation process in the response will be analyzed. Fig. 12. shows that the climate effects on the deposit are not remarkable. For instance, for a water table level of 5 m, the maximum acceleration response was 13.10 m/s^2 for 0 hours of evaporation and 13.10 m/s^2 for 87600 hours of evaporation. Analyzing the effect of the water table level, the results showed that the response is slightly different between the various water table levels. For example, for a water table level of 5 m, and an oscillator period of 0.36 seconds the acceleration spectrum de-amplifies from 19.05 m/s^2 to 12.74 m/s^2. On the other hand, this value de-amplifies to 13.22 m/s^2 when the water table level is 25 m. This means that when the deposit is dryer, the acceleration response is 3.76% higher than when the deposit is saturated. Fig. 4a shows the Fourier spectrum of the signal. Fig. 12 illustrates that the frequency content ranges from 2 Hz and 3 Hz, with a clear peak at 2.7 Hz. On the other hand, for values close to the natural frequency of the deposit, there is low-frequency content in comparison to the observed peak. In this manner, the de-amplification in the spectrum can be explained as a function of the decay in the frequency content. Fig. 12 shows that the seismic response depends on the frequency content of the signal.

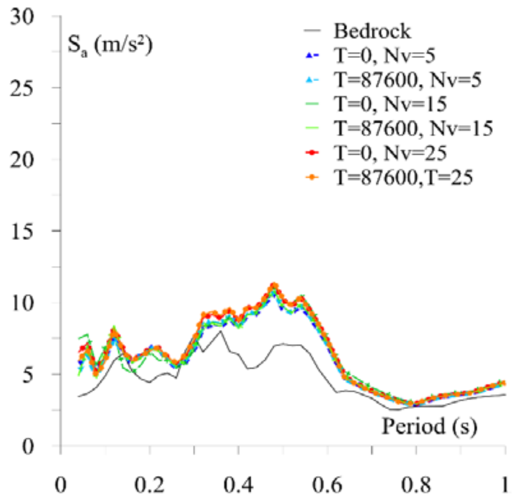

Fig. 12 1989 Loma Prieta (Gilroy N°1 E-W) acceleration response spectrum at the top of the deposit for different water table levels (i.e., 5, 15, 25m) and exposed to 0 and 87600 hours of evaporation.

6. CONCLUSIONS

This research presents the seismic response analysis of a soil column influenced by different water table levels (i.e., 5m, 15m, 25m) and subjected to different periods of evaporation (i.e., 0, 600, 87600 hours). To achieve this objective, a finite difference model was used to compute the water content profile under an evaporation flux. Then, a finite element model assessed the seismic response at the top of the soil column for different water tables and climatic conditions.

The finite-difference model showed that the environmental interaction does not have a remarkable change along with the soil depth after the first 5 meters. Likewise, the finite element model showed that there is no remarkable difference in the seismic response of the soil column after being exposed to climate conditions.

The results suggest that the water table level has a noteworthy effect on the dynamic response of the soil deposit. The results showed that the deposit with a lower water table has a higher seismic amplification. This research opens new possibilities in the research field, in which more seismic records should be analyzed, and epicenter proximity and frequency content should be considered. Also, this investigation could be replicated using different soils. This study showed that the water table influences the mechanical and dynamic behavior of soil deposits. Further investigations must be done since these aspects can impact the construction, reinforcement, and maintenance of structures.

7. REFERENCES

[1] Sánchez Sesma F. J., Rodríguez Zúñiga J. L., Pérez Rocha L. E., Cuevas A. and Suarez M., The seismic response of shallow alluvial valleys using a simplified model, in Memoria, 1992, p. 237–44.

[2] Villacreses J. P., Granados J., Caicedo B., Torres-Rodas P. and Yépez F., Seismic and hydromechanical performance of rammed earth walls under changing environmental conditions, Construction and Building Materials, vol. 300, p. 124-331, 2021.

[3] Villacreses J. P., Caicedo B., Caro S. and Yépez F., A novel procedure to determine shear dynamic modulus and damping ratio for partial saturated compacted fine-grained soils, Soil Dynamics and Earthquake Engineering, vol. 131, p. 106-129, 2020.

[4] McGann C. and Arduino P., Site response analysis of a layered soil column (total stress analysis), Opensees Example Wiki. University of Washington, 2010.

[5] Leong E.-C., Tripathy S. and Rahardjo H., Total suction measurement of unsaturated soils with a device using the chilled-mirror dew-point technique, Geotechnique, vol. 53, p. 173–182, 2003.

[6] Lysmer J. and Kuhlemeyer R. L., Finite dynamic model for infinite media, Journal of the Engineering Mechanics Division, vol. 95, p. 859–877, 1969.

[7] Lozada C., Caicedo B. and Thorel L., A new climatic chamber for studying soil–atmosphere interaction in physical models, International Journal of Physical Modelling in Geotechnics, vol. 19, p. 286–304, 2019.

[8] American Society of Civil Engineers, Minimum design loads and associated criteria for buildings and other structures, American Society of Civil Engineers, p. 203–204, 2017.

[9] Oh W. T. and Vanapalli S. K., Relationship between Poisson's ratio and soil suction for unsaturated soils, in Proc., 5th Asia-Pacific Conf. on Unsaturated Soils, p. 239-245, 2011.

[10] Bishop A. W., The principle of effective stress,Teknisk ukeblad, vol. 39, p. 859–863, 1959.

[11] Khalili N. and Khabbaz M. H., A unique relationship for χ for the determination of the shear strength of unsaturated soils, Geotechnique, vol. 48, p. 681–687, 1998.

[12] Burdzieva O. G., Zaalishvili V. B., Beriev O. G., Kanukov A. S. and Maysuradze M. V., Mining impact on environment on the North Ossetian territory, GEOMATE Journal, vol. 10, p. 1693–1697, 2016.

[13] Fathani T. F. and Wilopo W., Seismic microzonation studies considering local site effects for Yogyakarta City, Indonesia, GEOMATE Journal, vol. 12, p. 152–160, 2017.

[14] Zaalishvili V. B., Melkov D. A., Kanukov A. S., Dzeranov B. V. and Shepelev V. D., Application of microseismic and calculational techniques in engineering-geological zonation, GEOMATE Journal, vol. 10, p. 1670–1674, 2016.

[15] U. Berkeley, PEER Strong Ground Motion Databases. Pacific Earthquake Engineering Research Center, n.d. [Online]. Available: https://peer.berkeley.edu/peer-strong-ground-motion-databases. [Accessed november 2021].

[16] Fredlund D. G. and Xing A., Equations for the soil-water characteristic curve, Canadian geotechnical journal, vol. 31, p. 521–532, 1994.